RESEARCH ARTICLE

AMERICAN JOURNAL OF
medical genetics C
Seminars in Medical Genetics

WILEY

Clinical and genetic characteristics of Stargardt disease in a large Western China cohort: Report 1

Xiao Liu[1,2,3] | Xiaohong Meng[1] | Lizhu Yang[2,3] | Yanling Long[1] |
Yu Fujinami-Yokokawa[2,4,5] | Jiayun Ren[1] | Toshihide Kurihara[3] | Kazuo Tsubota[3] |
Kazushige Tsunoda[2] | Kaoru Fujinami[2,3,6,7] | Shiying Li[1] | East Asia Inherited
Retinal Disease Society Study Group

[1]Southwest Hospital/Southwest Eye Hospital, Third Military Medical University (Army Medical University), Chongqing, China

[2]Laboratory of Visual Physiology, Division of Vision Research, National Institute of Sensory Organs, National Hospital Organization Tokyo Medical Center, Tokyo, Japan

[3]Department of Ophthalmology, Keio University School of Medicine, Tokyo, Japan

[4]Department of Health Policy and Management, Keio University School of Medicine, Tokyo, Japan

[5]Department of Public Health Research, Yokokawa Clinic, Osaka, Japan

[6]UCL Institute of Ophthalmology, London, UK

[7]Moorfields Eye Hospital, London, UK

Correspondence
Kaoru Fujinami, 2-5-1, Higashigaoka, Meguro-ku, Laboratory of Visual Physiology, Division for Vision Research, National Institute of Sensory Organs, National Hospital Organization, Tokyo Medical Center, Tokyo 152-8902 Japan.
Email: k.fujinami@ucl.ac.uk

Shiying Li, Southwest Hospital/Southwest Eye Hospital, Third Military Medical University (Army Medical University), No. 30 Gaotanyan Street, Shapingba District, Chongqing 400038, P.R. China.
Email: shiying_li@126.com

Abstract

Stargardt disease 1 (STGD1) is the most prevalent retinal dystrophy caused by pathogenic biallelic *ABCA4* variants. Forty-two unrelated patients mostly originating from Western China were recruited. Comprehensive ophthalmological examinations, including visual acuity measurements (subjective function), fundus autofluorescence (retinal imaging), and full-field electroretinography (objective function), were performed. Next-generation sequencing (target/whole exome) and direct sequencing were conducted. Genotype grouping was performed based on the presence of deleterious variants. The median age of onset/age was 10.0 (5–52)/29.5 (12–72) years, and the median visual acuity in the right/left eye was 1.30 (0.15–2.28)/1.30 (0.15–2.28) in the logarithm of the minimum angle of resolution unit. Ten patients (10/38, 27.0%) showed confined macular dysfunction, and 27 (27/37, 73.7%) had generalized retinal dysfunction. Fifty-eight pathogenic/likely pathogenic *ABCA4* variants, including 14 novel variants, were identified. Eight patients (8/35, 22.8%) harbored multiple deleterious variants, and 17 (17/35, 48.6%) had a single deleterious variant. Significant associations were revealed between subjective functional, retinal imaging, and objective functional groups, identifying a significant genotype–phenotype association. This study illustrates a large phenotypic/genotypic spectrum in a large well-characterized STGD1 cohort. A

distinct genetic background of the Chinese population from the Caucasian population was identified; meanwhile, a genotype–phenotype association was similarly represented.

KEYWORDS

ABCA4, electroretinogram, multifocal electroretinogram, Stargardt disease

1 | INTRODUCTION

Stargardt disease (STGD1; MIM 248200), first described by Karl Stargardt, is an autosomal recessive retinal dystrophy caused by biallelic pathogenic variants in the *ABCA4* gene (ATP-binding cassette subfamily A member 4; MIM 601691) (Allikmets et al., 1997; K S, 1909). The *ABCA4* gene encodes a transmembrane rim protein (a member of the ABCA subfamily of ATP-binding cassette [ABC] transporters) in the outer segment discs of photoreceptors, which is involved in the active transport of retinoids from photoreceptors to retinal pigment epithelium (RPE) (Molday, 2015; Molday, Zhong, & Quazi, 2009; Quazi, Lenevich, & Molday, 2012). Failure of the transport results in accelerated deposition of a major lipofuscin fluorophore (N-retinylidene-N-retinylethanolamine; A2E) in the RPE, and A2E-associated cytotoxicity is believed to cause RPE dysfunction with subsequent photoreceptor cell loss over time (Chen et al., 2012; Maeda, Maeda, Golczak, & Palczewski, 2008; Molday, Rabin, & Molday, 2000; Tsybovsky, Molday, & Palczewski, 2010).

STGD1, with a prevalence of 1 in 8,000–10,000, is one of the most common inherited macular dystrophies with characteristic features, including macular atrophy and yellow–white flecks at the level of the RPE at the posterior pole (Gill, Georgiou, Kalitzeos, Moore, & Michaelides, 2019; Liu, Fujinami, Yang, Arno, & Fujinami, 2019; Rahman, Georgiou, Khan, & Michaelides, 2020; Tanna, Strauss, Fujinami, & Michaelides, 2017). Onset is most common in teens but variable, and a severe and progressive phenotype has been associated with childhood-onset and a mild phenotype with late-onset (Fujinami et al., 2011; Fujinami, Lois, Davidson, et al., 2013; Fujinami, Lois, Mukherjee, et al., 2013; Fujinami, Sergouniotis, Davidson, Mackay, et al., 2013; Fujinami, Sergouniotis, Davidson, Wright, et al., 2013; Fujinami et al., 2014; Fujinami et al., 2015; Fujinami-Yokokawa et al., 2019; Georgiou et al., 2020; Gill et al., 2019; Khan et al., 2018; Liu et al., 2019; Rahman et al., 2020; Singh, Fujinami, Chen, Michaelides, & Moore, 2014; Tanna et al., 2017, 2019). The vast phenotypic heterogeneity and variable severity of *ABCA4*-associated retinopathy are well-known and encompass macular atrophy without flecks, bull's-eye maculopathy, fundus flavimaculatus (retinal flecks without macular atrophy), a foveal sparing phenotype, cone-rod dystrophy, and "retinitis pigmentosa"; genotype–phenotype associations have been reported based on clinical severity and the presence of deleterious variants (Fujinami et al., 2011, 2014, 2015; Fujinami, Lois, Davidson, et al., 2013; Fujinami, Lois, Mukherjee, et al., 2013; Fujinami, Sergouniotis, Davidson, Mackay, et al., 2013; Fujinami, Sergouniotis, Davidson, Wright, et al., 2013; Georgiou et al., 2020; McBain, Townend, & Lois, 2012; Singh et al., 2014; Strauss et al., 2019; Tanna et al., 2017, 2019; Testa et al., 2014).

Cross-sectional and longitudinal studies in large cohorts focusing mainly on the European population have been widely performed (Fujinami, Zernant, et al., 2013; Fujinami et al., 2019; Kong et al., 2016, 2018; Schonbach et al., 2017; Schulz et al., 2017; Strauss et al., 2016; Strauss, Munoz, Ho, Jha, Michaelides, Cideciyan, et al., 2017; Strauss, Munoz, Ho, Jha, Michaelides, Mohand-Said, et al., 2017; Strauss et al., 2019). Clinical trials of treatments including visual cycle modification (ClinicalTrials.gov Identifier: NCT02402660), gene augmentation therapy (ClinicalTrials.gov Identifier: NCT01367444), and stem cell therapy (ClinicalTrials.gov Identifier: NCT01469832) are ongoing mainly in Europe/North America (Charbel Issa, Barnard, Herrmann, Washington, & MacLaren, 2015; Hussain, Ciulla, et al., 2018; Hussain, Gregori, Ciulla, & Lam, 2018; Kubota et al., 2012; Kubota, Calkins, Henry, & Linsenmeier, 2019; Mehat et al., 2018; Rosenfeld et al., 2018; Schwartz et al., 2012, 2015). However, large cohort studies based on standardized clinical and genetic diagnostic criteria in the Asian population are very limited.

Therefore, the purpose of this study was to characterize the comprehensive phenotypic and genotypic features of Chinese patients with STGD1 in a large cohort in preparation for therapeutic trials. A systematic review of *ABCA4* variants was performed to delineate the genetic spectrum in the Chinese population.

2 | METHODS

The procedures applied in this study were approved by the local ethics committee of Southwest Eye Hospital, Third Military Medical University (Army Medical University), Chongqing, China (reference number: 73981486-2), and all procedures were performed in accordance with the Declaration of Helsinki.

2.1 | Participants

Patients were recruited at the Southwest Eye Hospital, Third Military Medical University (Army Medical University), Chongqing, China, from 2013 to 2019 according to the following criteria mainly described in a

AMERICAN JOURNAL OF
medical genetics
Seminars in Medical Genetics

previous publication: (Strauss et al., 2016) patients with multiple disease-causing variants in the ABCA4 gene or patients with one disease-causing variant and typical clinical findings (i.e., macular atrophy with flecks) for STGD1. Clinical and molecular genetic diagnoses were confirmed by three senior doctors (XM, KF, SL). Patients who had other ocular diseases, such as choroidal neovascularization, glaucoma, and diabetic retinopathy, or were undergoing treatments/therapeutic trials were excluded.

2.2 | Clinical investigations

Detailed history and comprehensive ophthalmological examinations were conducted, including best-corrected decimal visual acuity (BCVA), dilated ophthalmoscopy, color fundus photography (non-myd WX 3D, Kowa, Tokyo, Japan), fundus autofluorescence imaging (FAF; excitation light: 488 nm, barrier filter: 500 nm, field of view: 30° × 30°, 55° × 55°; Spectralis, Heidelberg Engineering, Heidelberg, Germany), optical coherence tomography (OCT; Spectralis, Heidelberg Engineering; and ZEISS CIRRUS, Carl Zeiss Meditec AG, Oberkochen, Germany), and microperimetry (MP, MAIA, Padoba, Italy). BCVA was converted to the equivalent value in the logarithm of the minimum angle of resolution (LogMAR) unit, and low visual categories, including counting finger (CF) and hand movement (HM), were valued at 1.98 and 2.28, as reported previously (Fujinami, Lois, Mukherjee, et al., 2013; Lange, Feltgen, Junker, Schulze-Bonsel, & Bach, 2009).

Full-field electroretinograms (ffERGs; Diagnosys LLC, Lowell, MA) were recorded in accordance with the international standards of the International Society for Clinical Electrophysiology of Vision (ISCEV) (McCulloch et al., 2015a; McCulloch et al., 2015b) Multifocal ERGs (mfERGs) were recorded with a VERIS imaging system (EDI, San Mateo, CA) in accordance with the ISCEV standard protocol, and eyes with stable fixation during the mfERG recording were selected for further analyses (Hood et al., 2012).

Fundus appearance, FAF findings, OCT findings, and ffERG findings were classified based on specific features according to previous publications (Table 1) (Fujinami, Lois, Davidson, et al., 2013; Fujinami, Lois, Mukherjee, et al., 2013; Lois, Holder, Bunce, Fitzke, & Bird, 2001; Testa et al., 2014).

Fundus appearance was classified into four grades (grade 3 has three subgroups) based on the presence and location of central (macular), RPE atrophy and yellowish-white flecks. Grade 1: normal fundus; grade 2: macular and/or peripheral flecks without central atrophy; grade 3a: central atrophy without flecks; grade 3b: central atrophy with macular and/or peripheral flecks; grade 3c: paracentral atrophy with macular and/or peripheral flecks, without central atrophy; grade 4: multiple extensive atrophic changes of the RPE, extending beyond the vascular arcades.

Patterns of AF signal of the central retina and background was classified into three types. Type 1: localized low AF signal at the fovea surrounded by a homogeneous background, with/without perifoveal foci of high or low AF signal; Type 2: localized low AF signal at the

TABLE 1 Classification for fundus appearance, fundus autofluorescence images, optical coherence tomographic images, and full-field electroretinograms in Stargardt disease (STGD1)

	Fundus grade		AF pattern		OCT category		FfERG group
Grade 1	Normal fundus	Pattern 1	Localized low AF signal at the fovea surrounded by a homogeneous background with/without perifoveal foci of high or low signal	Category I	EZ preservation in the fovea	Group 1	Macular dysfunction (normal full-field ERG)
Grade 2	Macular and/or peripheral flecks without central atrophy	Pattern 2	Localized low AF signal at the macula surrounded by a heterogeneous background and widespread foci of high or low AF signal extending anterior to the vascular arcades	Category II	EZ loss in the foveal area	Group 2	Macular dysfunction with generalized cone dysfunction
Grade 3a	Central atrophy without flecks	Pattern 3	Multiple areas of low AF signal at posterior pole with a heterogeneous background and/or foci of high or low signal	Category III	Extensive loss of EZ line	Group 3	Macular dysfunction with generalized cone and rod dysfunction
Grade 3b	Central atrophy with and/or peripheral flecks						
Grade 3c	Para-central atrophy with macular and/or peripheral flecks, without a central atrophy						

Abbreviations: AF, autofluorescence; ERG, electroretinogram; EZ, photoreceptor ellipsoid zone; RPE, retinal pigment epithelium.

macula surrounded by a heterogeneous background, and widespread foci of high or low AF signal extending anterior to the vascular arcades; Type 3: multiple areas of low AF signal at the posterior pole with a heterogeneous background, with/without foci of high or low AF signal.

Morphological changes of photoreceptor ellipsoid zone (EZ) in the central retina detected by OCT were classified into three categories. Category I: preserved EZ in the fovea; category II: loss of EZ in the foveal; category III: extensive loss of EZ.

Based on the ffERGs findings, patients were assigned to three ffERG groups. Group 1: normal ffERG responses; group 2: generalized cone ERG abnormality with normal rod responses; group 3: generalized cone and rod ERG abnormality.

The median P1 amplitude decline rates [(medical value of normative range − P1 value)/medical value of normative range] of mfERG rings 1 and 2, rings 3 and 4, and rings 5 and 6 were calculated for the analyses.

One eye was randomly selected using random.org software (https://www.random.org/) for the classification and analysis of fundus appearance, FAF images, OCT images, and ffERGs.

2.3 | Classification of phenotypic severity

The overall classification of phenotypic severity was performed based on the following clinical parameters mainly according to a previous publication: (Fujinami, Sergouniotis, Davidson, Mackay, et al., 2013) age of onset, BCVA (LogMAR), fundus grade, AF pattern, OCT category, and ffERG grouping (group 1: mild phenotype; group 2: moderate phenotype; and group 3: severe phenotype) (Table 2).

2.4 | Variant detection

After obtaining informed consent, peripheral venous blood samples were collected from all subjects and unaffected family members (if available) for co-segregation analysis. Genomic DNA was isolated by a standard procedure. Either eye gene-enriched (from 36 to 450 target genes) panel-based next-generation sequencing (NGS) or whole exome sequencing (WES) was performed. Sanger bi-directional sequencing was conducted to confirm the rare candidate variants (allele frequency: less than 1.0% of the general population) and to perform the co-segregation analysis. Disease-causing variants were determined from the detected variants while considering the clinical findings of the affected subjects, the pattern of inheritance in the pedigree, and the results of the co-segregation analysis.

2.5 | *In silico* molecular genetic analyses

Sequence variant nomenclature was performed according to the guidelines of the Human Genome Variation Society (HGVS; https://varnomen.hgvs.org) with Mutalyzer (https://mutalyzer.nl/). All variants were analyzed using the following databases and prediction software: GnomAD (http://gnomad.broadinstitute.org/), 1,000 Genome (https://www.internationalgenome.org/), MutationTaster (http://www.mutationtaster.org/), FATHMM (http://fathmm.biocompute.org.uk/9), SIFT (https://www.sift.co.uk/), PROVEAN (http://provean.jcvi.org/index.php), Polyphen2 (http://genetics.bwh.harvard.edu/pph2/) Phylop and Phastcons from the University of California Santa Cruz database (https://genome.ucsc.edu/index.html), Human Splicing Finder (HSF, http://www.umd.be/HSF3/), Database Splicing Consensus Single Nucleotide Variant (dbscSNV, http://sites.google.com/site/jpopgen/dbNSFP), and Ensembl Variant Effect Predictor (VEP, http://grch37.ensembl.org/info/docs/tools/vep/index.html). Missense variants with predicted splice site alterations were treated as deleterious variants.

In accordance with the American College of Medical Genetics (ACMG) guidelines, variants were classified as pathogenic, likely pathogenic, uncertain significance (VUS), likely benign, or benign (Richards et al., 2015).

2.6 | Genotype group classification

The patients harboring multiple pathogenic or likely pathogenic variants were classified into three genotype groups based on the

TABLE 2 Classification of phenotypic severity

	Onset of disease (years)	BCVA (logMAR) in the better eye	Fundus grade	AF type	OCT category	FfERG group
Mild phenotype (group 1)	Later onset (≥40)	<0.78	1	1	1	1
Moderate phenotype (group 2)	Patients who did not meet at least two criteria of either mild phenotype or severe phenotype were classified into the moderate phenotype subgroup.					
Severe phenotype (group 3)	Early onset (<10)	>1.0	4	3	3	3

Note: For the purpose of this study, patients who met at least three criteria of mild phenotype were classified into the mild phenotype subgroup and those who had at least three features of severe phenotype were classified into the severe phenotype subgroup. Patients who met both at least three features of mild phenotype and at least three features of severe phenotype were classified into group 2 (moderate phenotype).
Abbreviation: BCVA, best-collected visual acuity in the LogMAR VA in the logarithm of the minimum angle of resolution (logMAR) unit.

number/presence of deleterious variants according to previous reports: (Fujinami et al., 2015; Fujinami et al., 2019; Fujinami, Lois, Mukherjee, et al., 2013; Kong et al., 2018) Sequence variants which presumably lead loss-of-function (frameshift, stop-gained, splice site alteration) are defined as null variants. Variants that are not likely to have null-effects such as missense variants or in-frame alteration were defined as non-null variants. Group A: patients with multiple definite or likely null variants; group B: patients with one null variant and one or more non-null variant(s); and group C: patients with multiple non-null variants.

2.7 | A systematic review of *ABCA4* variants

A literature review of *ABCA4*-associated retinal disease in the Chinese population was performed. Peer-reviewed published papers were searched with the terms Chinese, ABCA4, and Stargardt disease; articles reporting at least 10 patients were surveyed.

In silico molecular genetic analyses were performed, and assessment of pathogenicity was performed with the same method applied in the current study cohort. Prevalent variants based on allele frequency in the affected group cohort were calculated for each study and the total study.

2.8 | Statistical analysis

Data analyses were performed using SPSS version 23.0 (IBM Corp, Armonk, NY). The age at baseline examination, age of onset, BCVA (in the LogMAR unit), MP threshold (4–2), and amplitude of P1 of mfERG were compared between fundus, FAF, OCT, ffERG, and genotype groups with Mann–Whitney U tests. An association between phenotypic severity classification and genotype group classification was investigated by Fisher's exact test. p values <.05 were considered statistically significant.

3 | RESULTS

3.1 | Demographics

A total of 42 unrelated patients (28 men and 14 women) were included in this study. Two patients (A002 and A035) were from consanguineous families (Figure 1). The detailed clinical findings are presented in Data S1.

The patients mostly originated from the western part of China (32/42, 76.2%). The median age at baseline examination was 29.5 years (range, 12–72), and the median age of onset was 10 years (range, 5–52). The median BCVA, available in 40 patients, was 1.30 (range, 0.15–2.28) for the right eye and 1.30 (range, 0.15–2.28) for the left eye.

3.2 | Retinal images

The fundus photographs, autofluorescence images, and OCT images for three representative patients are shown in Figure 2.

Fundus photographs were obtained in 41 patients (Data S1). All these patients were classified into grades 3b and 4 according to their fundus appearance. No asymmetric grades were observed. There were 22 patients (22/41, 53.7%) in grade 3b and 19 (19/31, 61.3%) in grade 4 (Figure S1). There was a significant difference in BCVA between grades 3b and 4 (p = .0004; Data S1 and Figure S2). FAF images were obtained in 41 patients (Data S1). There were 10 patients (10/41, 24.4%) with a type 1 AF pattern, 18 (18/41, 43.9%) with a type 2 AF pattern, and 13 (13/41, 31.7%) with a type 1 AF pattern (Figure S1). No asymmetric types were observed. There were significant differences in age and BCVA between patients with AF type 1 and type 3 patterns (p = .0111, p = .0167; Data S1, Figure S2). OCT images were obtained in 39 patients (Data S1). There were eight patients (8/39, 20.5%) with category II OCT findings and 31 (31/39, 79.5%) with category III OCT findings (Figure S1). One patient (A013) showed an asymmetric classification with category II of the right eye and category III of the left eye. There was a significant difference in BCVA between patients with OCT category II and category III (p = .000086; Data S1, Figure S2).

3.3 | Retinal function and microperimetry

The traces of ffERGs and mfERGs and MP results for three representative patients are presented in Figure 3.

FfERGs were recorded in 37 patients (Data S1). There were 10 patients (10/37, 27.0%) in ffERG group 1, four patients (4/37, 10.8%) in group 2, and 23 patients (23/37, 62.2%) in group 3 (Figure S1). No asymmetric ffERG groups were observed. There were significant differences in age between patients in group 1 and group 2 as well as in BCVA between patients in ffERG group 1 and group 3 (p = .034, p = .002; Data S1 and Figure S2).

MfERGs were obtained in 30 patients, and 40 eyes from 24 patients with stable fixation were analyzed (Data S1). There were 15 eyes in ffERG group 1, seven eyes in ffERG group 2, and 18 eyes in ffERG group 3. The median P1 amplitude decline rates of mfERG rings 1 and 2, 3 and 4, and 5 and 6 in the ffERG groups are summarized in Table S2. There were significant differences in terms of the P1 amplitude decline rate of rings 1 and 2, rings 3 and 4, and rings 5 and 6 between ffERG group 1 and group 3 (p = .0033, p = .000005, p = .00000009). Significant differences were found in terms of the P1 amplitude decline rate for rings 3 and 4 and rings 5 and 6 between ffERG group 2 and group 3 (p = .0012, p = .0004). Significant differences in terms of the P1 amplitude decline rate of rings 5 and 6 were observed between ffERG group 1 and group 2 as well (p = .059, Figure S3).

MP was performed in 23 patients. All 23 patients showed preferred retinal locus (PRL)-fixation changes. There were 12 eyes in ffERG group 1, eight eyes in ffERG group 2, and 25 eyes in ffERG

FIGURE 1 Pedigree charts of 42 families with Stargardt disease. An arrow (→) indicates the proband. A filled shape indicates the affected individual, and a cross (✕) indicates the family members who underwent genetic testing. Square, male; circle, female. The generation number is shown on the left

group 3. The median average sensitivity threshold of the macula was 19.8 dB (range, 0.0–29.2), 15.1 dB (range, 0.0–25.8), and 0.0 dB (range, 0.0–18.9) in ffERG group 1, group 2, and group 3, respectively.

There was a significant difference between ffERG group 1 and group 3 as well as between ffERG group 2 and group 3 (p = .000003, p = .076; Figure S4).

Fundus	FAF	OCT
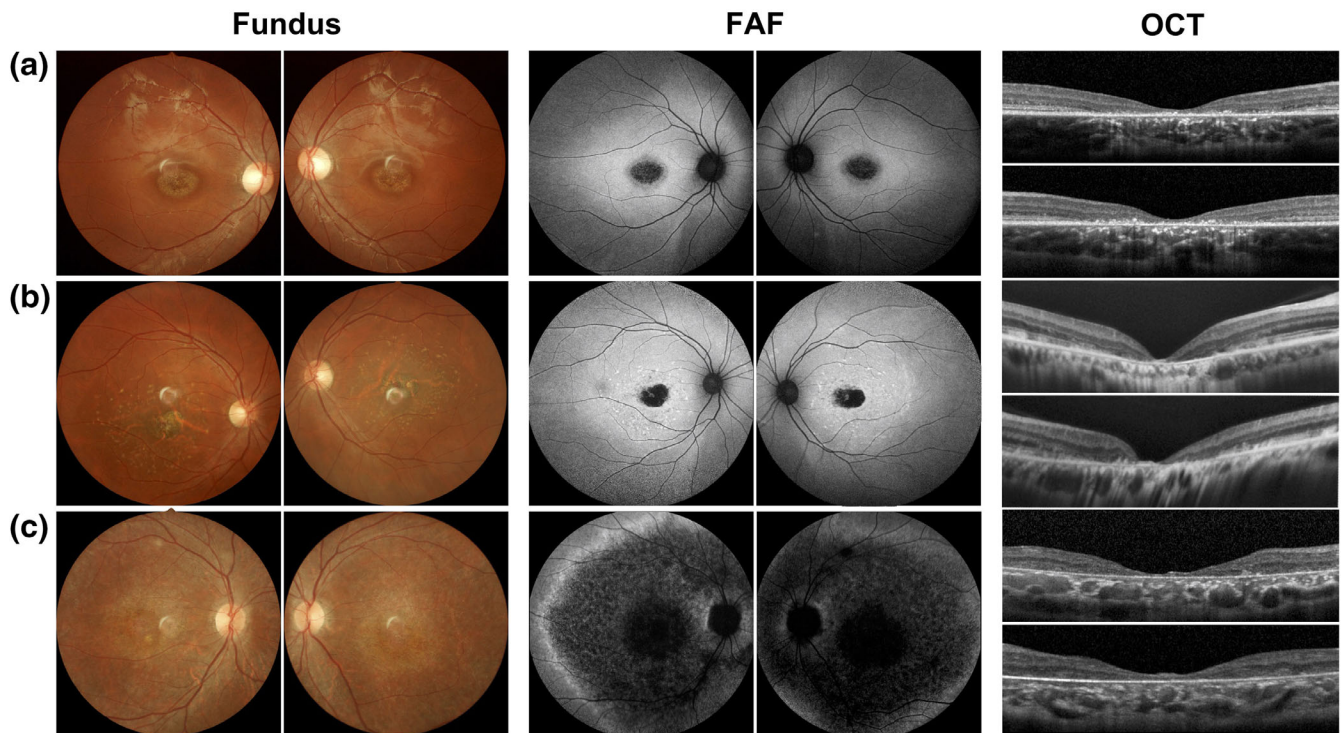
FIGURE 2 Color fundus photographs, fundus autofluorescence images, and optical coherence tomographic images from three representative patients with Stargardt disease (STGD1). (a) A002 (15-year-old female; onset at 9 years; best-corrected visual acuity of 0.82/0.82 in the logMAR unit for the right/left eye; [c.6563T>C (p.Phe2188Ser) and c.5318C>T (p.Ala1773Val)]; genotype group C. Fundus photographs show a central atrophy without flecks at the posterior. Fundus autofluorescence (FAF) images identify an area of low AF signal located at the fovea with homogenous background. Optical coherence tomographic (OCT) images demonstrate outer retinal disruption at the macula. (b) A040 (34-year-old male; onset at 10 years; best-corrected visual acuity of 1.00/1.00 in the logMAR unit for the right/left eye; [c.6563T>C (p.Phe2188Ser)] and [c.303-2A>G]; genotype group B). Fundus photographs show a central atrophy surrounded by flecks at the posterior pole; FAF images identify an area of low AF signal located at the macula with numerous foci of high AF density at the posterior pole; OCT images demonstrate outer retinal disruption at the macula. (c) A008 (22-year-old male; onset at 10 years; best-corrected visual acuity of 2.28/1.98 in the logMAR unit for the right/left eye; [c.1761-2A>G] and [c.2424C>G (p.Tyr808ter)]; genotype group A). Fundus photographs show multiple extensive atrophic changes in the retinal pigment epithelium (RPE), extending beyond the vascular arcades. FAF images identify multiple areas of low AF signal at posterior pole with a heterogeneous background. OCT images demonstrate widespread outer retinal disruption

3.4 | Phenotypic severity

Phenotype severity classification was available in 42 patients (Data S1). There was no patient (0/42, 0.0%) with a mild phenotype, 16 patients (16/42, 38.1%) with a moderate phenotype and 26 (26/42, 61.9%) with a severe phenotype.
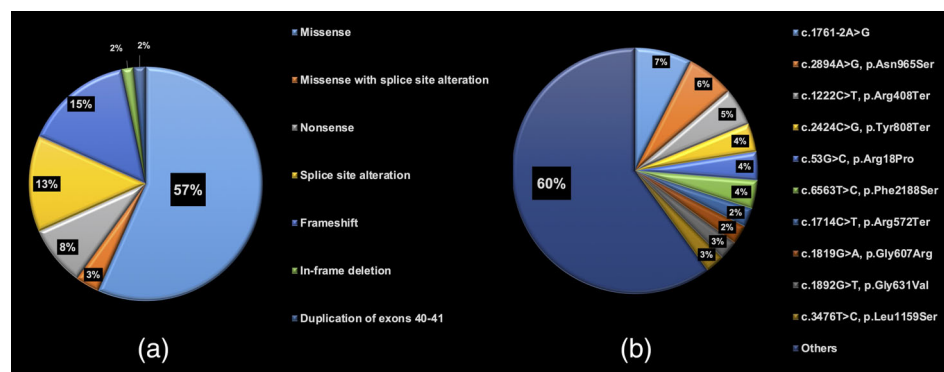
3.5 | *ABCA4* variants

Genetic results were obtained in all 42 unrelated patients: 34 patients underwent panel-based NGS, and eight patients underwent WES. Two *ABCA4* variants were detected in 39 patients, while two patients (A003 and A005) had a single variant and one (A022) had three variants. Co-segregation analyses were available in 32 families: 26 probands with confirmed biallelic variants with genetic results of parents or certain family members; six probands with partially segregated results of a single parent or relatives; and 10 probands with no available data (Data S1 and Figure 1).

The detailed molecular genetic results are provided in Table S3. In total, 60 *ABCA4* variants were identified in this study, including 36 missense variants (36/60, 60.0%), nine frameshift alterations (9/60, 15.0%), eight splice site alterations (13.3%), five nonsense variants (5/60, 8.3%), one in-frame deletion (1/60, 1.7%) and one duplication of exons 40–41 (1/60, 1.7%) (Figure 4). Two missense variants (c.6284A>T (p.Asp2095Val) and c.6283G>C (p.Asp2095His)) located around the end of exon 46 was predicted to cause splice site alterations. Fourteen novel *ABCA4* variants were first reported in this study (Table S3). Two de novo *ABCA4* variants were identified in two families: c.5019del (p.Val1673CysfsTer2) (A022) and c.1761-2A>G (A023) (Figure 1). There are three variants identified in the homozygous status: c.1222C>T (p.Arg408Ter) (A020); c.53G>C (p.Arg18Pro) (A030); and c.1714C>T (p.Arg572Ter) (A045).

The most prevalent six variants were c.1761-2A>G (6/80 alleles, 8%); c.2894A>G (p.Asn965Ser) (5/80 alleles, 6%); c.1222C>T (p.Arg408Ter) (4/80 alleles, 5%); c.2424C>G (p.Tyr808Ter) (3/80 alleles, 4%); c.53G>C (p.Arg18Pro) (3/80 alleles, 4%); and c.6563T>C (p.Phe2188Ser) (3/80 alleles, 4%) (Figure 4).
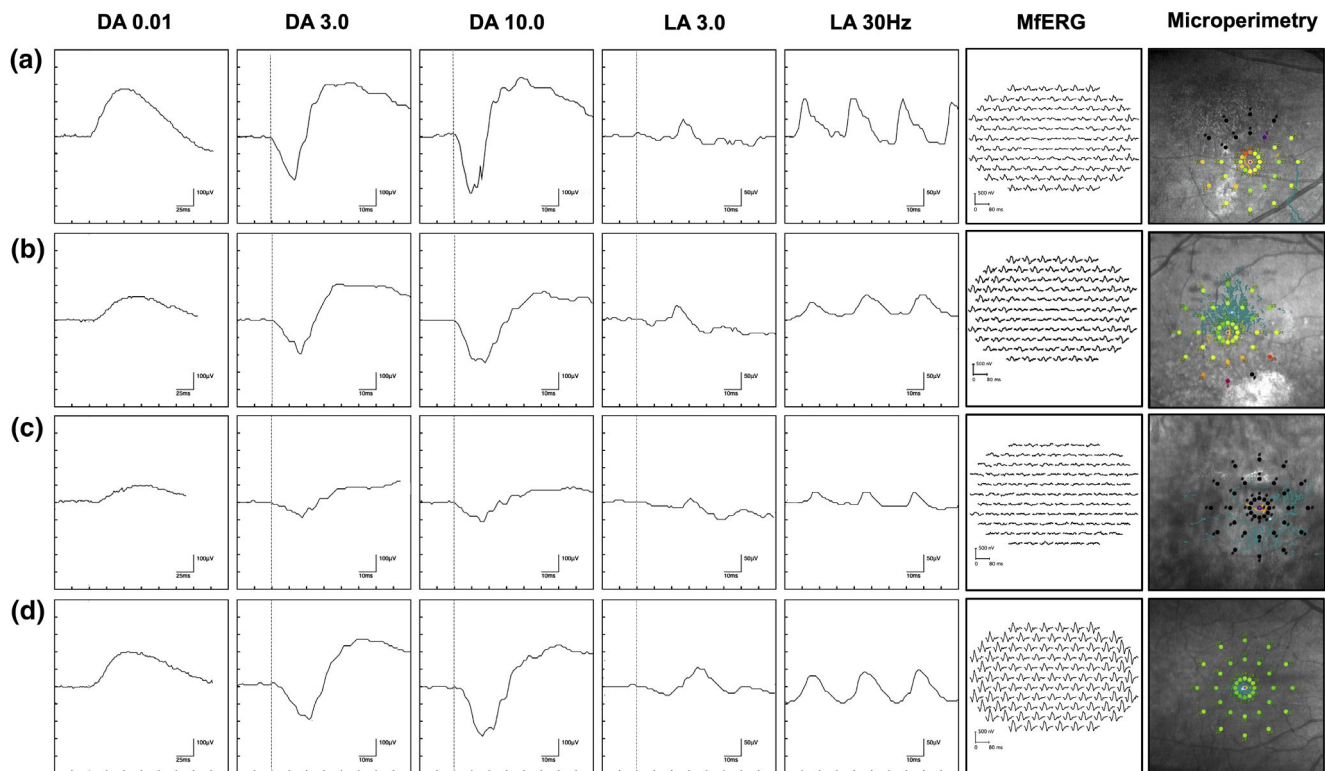
FIGURE 3 Full-field electroretinograms (ffERGs), multifocal ERGs (mfERGs), and microperimetry from three representative patients with STGD1. (a) A002 (full-field electroretinogram group 1; ffERG group 1). FfERGs demonstrate normal dark-adapted (DA) responses (DA 0.01, DA 3.0, DA 10.0) and normal light-adapted (LA) responses (LA 3.0, LA 3.0 30 Hz flicker). Multifocal ERGs (mfERGs) detect severely decreased responses in the central area (rings 1–2) and mildly decreased responses in rings 3–6. Microperimetry (MP) presents a preferred retinal locus (PRL) located at the nasal fovea, and the average threshold at the macula is 26.4 dB. (b) A040 (ffERG group 2). FfERGs demonstrate normal DA responses and mildly decreased LA responses. MfERGs detect severely decreased responses in rings 1–4 and mildly decreased responses in rings 5–6. MP present a PRL located at the superior fovea, and the average threshold at the macula is 25.8 dB. (c) A008 (ffERG group 3). FfERGs demonstrate moderately decreased DA responses and moderately decreased LA responses. MfERGs detect severely decreased responses over the recorded area. MP presents the average threshold of 0 dB. (d) Normal reference. Data from a normal subject are shown for reference

FIGURE 4 Distribution of detected *ABCA4* variants in a Western China cohort. (a) Type of detected variants. There were 36 missense variants (36/60, 60.0%), nine frameshift alterations (9/60, 15.0%), eight splice site alterations (13.3%), five nonsense variants (5/60, 8.3%), one in-frame deletion (1/60, 1.7%), and one duplication of exons 40–41 (1/60, 1.7%) identified in this study. Two missense variants (c.6284A>T (p.Asp2095Val) and c.6283G>C (p.Asp2095His)) are predicted to cause splice site alterations. (b) Allele frequency of detected variants. The distribution of 10 relatively prevalent variants identified in at least two families is demonstrated. The variants with allele frequencies less than 2% are summarized into others

The allele frequency provided by gnomAD in the total/East Asian general population for these six prevalent variants was 0.0004092%/0% for c.1761-2A>G; 0.013%/0% for p.Asn965Ser; 0.001625%/0.005% for p.Arg408Ter; 0%/0% for p.Tyr808Ter; 0%/0% for p.Arg18Pro; and 0.0008122%/0.005% for p.Phe2188Ser. The allele frequency provided by gnomAD in the total/East Asian

general population and this study for each variant was performed (Table S4).

Pathogenicity classification based on the ACMG guidelines was available for 60 detected variants. There were 24 variants classified as pathogenic, 34 as likely pathogenic, one as a variant of uncertain significance (VUS) (c.4577C>T (p.Thr152Met); A027), and one as a likely benign variant (c.3547G>T (p.Gly1183Cys); A015) (Table S3).

3.6 | Genotype classification

Genotype group classification was performed in 36 patients harboring multiple pathogenic or likely pathogenic variants. There were eight patients (8/36, 22.2%) with genotype A, 17 patients (47.2%) with genotype B, and 11 patients (30.5%) with genotype C (Figure S1).

The median age, age of onset, and BCVA in genotype A was 29.0 years (range, 18–52), 10.0 years (range, 8–14), and 1.64 in the LogMAR unit (range, 1.00–2.28), respectively. The median age, age of onset, and BCVA in genotype B was 34.0 years (range, 12–72), 10.0 years (range, 5–49), and 1.30 in the LogMAR unit (range, 0.15–1.98), respectively. The median age, age of onset, and BCVA in genotype C was 28.0 years (range, 15–46), 10.0 years (range, 8–20), and 1.00 in the LogMAR unit (range, 0.40–1.30), respectively. There was a significant difference in BCVA between genotype group A and genotype group C (p = .0052, Table S5).

3.7 | Genotype–phenotype association

An association between phenotypic severity and genotype group was investigated in 36 patients. The number of phenotypically moderate patients in genotype groups A, B, and C was zero, five, and seven, respectively (0%, 29.4%, 63.6%). The number of phenotypically severe patients in genotype groups A, B, and C was eight, twelve, and four, respectively (100%, 70.6%, 36.4%). A statistically significant association between phenotypic severity and genotype group was revealed (p < .05) (p = .01, Table 3 and Figure 5).

3.8 | A systematic review of *ABCA4* variants

Four articles were selected for the analysis of Chinese ABCA4 variants (Table S6). A total of 212 *ABCA4* variants were identified in these four studies, including 114 missense, 36 splice site alterations, 31 nonsense variants, 25 frameshift variants, 3 synonymous variants, and 3 others (Table S7). Out of 212 *ABCA4* variants, 150 were classified as pathogenic or likely pathogenic according to the ACMG guidelines. Prevalent variants in total were c.101_106del (p.Ser34_Leu35del) (allele frequency of 6%); c.2894A>G (p.Asn965Ser) (allele frequency of 4%); c.6563T>G (p.Phe2188Ser) (allele frequency of 4%); and c.2424C>G (p.Tyr808Ter) (allele frequency of 3%) (Figure S5).

Prevalent variants in each study were c.101_106del (p.Ser34_Leu35del); c.4773+1G>T; c.5646G>A (p.Met1882Ile); and c.1804C>T (p.Arg602Trp) in study 1 (Xin et al., 2015; N = 33). c.2424C>G (p.Tyr808Ter); c.6563T>G (p.Phe2188Ser); c.101_106del (p.Ser34_Leu35del); and c.2894A>G (p.Asn965Ser) in study 2 (Jiang, Pan, Xu, Tian, & Li, 2016; N = 161). c.101_106del (p.Ser34_Leu35del); c.2894A>G (p.Asn965Ser); c.6563T>G (p.Phe2188Ser); and c.1819G > A (p.Gly607Arg) in study 3 (Hu, J-k, Gao, Qi, & Wu, 2019; N = 153) and c.2894A>G (p.Asn965Ser); and c.101_106del (p.Ser34_Leu35del) in study 4 (Dan, Huang, Xing, & Shen, 2019; N = 12) (Table S6). Basically, those articles mainly focused on genotype analysis. There were little phenotypic data such as retinal image and electrophysiology was available and the correlation between phenotype and genotype was not analyzed.

4 | DISCUSSION

Detailed clinical and genetic characteristics are illustrated in a Western China cohort of 42 probands with STGD1. A wide disease spectrum both in phenotype and genotype was determined in a large Chinese cohort, identifying no patient with a mild phenotype, 38.1% with a moderate phenotype, and 61.9% with a severe phenotype associated with genetic severity.

To the best of the authors' knowledge, this study is the first to comprehensively reveal the demographic, morphological, and functional features of patients with STGD1 in a large molecularly confirmed cohort, which enabled an elucidation of the genotype–phenotype association in the Chinese population.

The median onset in our cohort (10.0 years) was earlier than that in the large prospective international STGD1 cohort (21.8 years for the retrospective cohort and 22.3 years for the prospective cohort in the ProgStar studies) or other reports from Europe (approximately 20 years) (Fujinami, Lois, Davidson, et al., 2013; Fujinami, Lois,

TABLE 3 Association between genotype group and phenotypic severity

		Phenotypic severity		
		Group 1 (mild)	Group 2 (moderate)	Group 3 (severe)
Genotype group	Group A (multiple deleterious)	0	0	8
	Group B (one deleterious)	0	5	12
	Group C (multiple missense)	0	7	4

Note: A statistically significant association was reveled between genotype group classification and phenotypic severity classification (p = .014; p < .05, Fisher exact test).
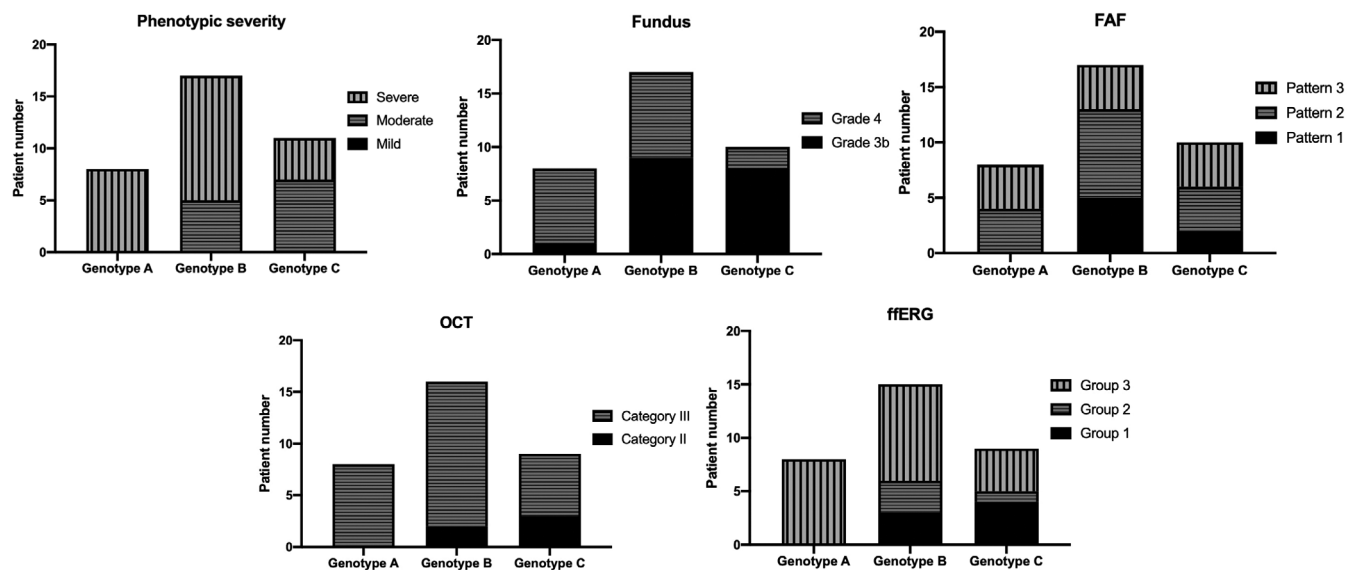
FIGURE 5 Clinical classification for each genotype group. Clinical classifications of phenotypic severity, fundus grades, FAF types, ffERG groups, and OCT categories for each genotype group are shown in bar graphs. There was a significant association between phenotypic severity and genotype group classification

Mukherjee, et al., 2013; Fujinami, Zernant, et al., 2013; Strauss et al., 2016). These findings were associated with a high proportion of severe phenotype in our cohort. The higher proportion of genotype group A with multiple deleterious variants (22%) in our cohort than in the other cohort (ProgStar cohort; 6%) supports this important fact (Fujinami et al., 2019; Kong et al., 2018). A similar proportion of genotype group A to our cohort was also found in the childhood-onset Stargardt disease cohort in the United Kingdom (Fujinami et al., 2015; Georgiou et al., 2020; Tanna et al., 2019).

Functional assessment is crucial in STGD1, since it provides not only distribution of the affected retinal area and affected systems (cone or rod) but also a prognostic value (Fujinami, Lois, Davidson, et al., 2013; Lois et al., 2001). The most severe functional phenotype (ffERG group 3: generalized cone and rod dysfunction) showed significant progression (over 50% loss of function) during the 10-year follow-up; (Fujinami, Lois, Davidson, et al., 2013) thus, careful observation and constructive intervention (if possible) are needed during the course in approximately 60% of our cohort. Spatial functional assessment with mfERGs detected a trend of an extended reduction in P1 amplitude according to the severity of ffERGs. This new approach could provide more detailed assessment/monitoring of retinal function in patients with STGD1 in natural history studies and therapeutic trials.

The combination of subjective and objective functional assessments provided useful information in our study. MP, a procedure to assess retinal sensitivity by monitoring the fundus, detected a lack of fixation stability with lower sensitivity thresholds, in keeping with previous reports (Sasso et al., 2017; Schonbach et al., 2017, 2020; Tanna et al., 2018, 2019). In addition, the severity of retinal sensitivity loss was associated with the severity of generalized retinal functional loss detected by ffERG, which suggests that the combination of subjective

and objective functional assessments could explain the key symptom of poor fixation and blurred central vision often associated with peripheral functional impairment.

Fourteen detected *ABCA4* variants (14/60, 23.3%) identified in our cohort have never been reported. This fact implies that the genetic background of the Chinese population was distinct from that of other populations. In addition, the three most prevalent variants (c.1761-2A>G; c.2894A>G (p.Asn965Ser); and c.1222C>T (p.Arg408Ter)) detected in our cohort were completely different from the three most prevalent variants (c.5882G>A (p.Gly1961Glu); c.2588G>C (p.Gly863Ala); and c.5461–10T>C) in the ProgStar study (Fujinami et al., 2019). In contrast to this regional/ethnic variation, genotype–phenotype associations were similarly identified in our cohort compared with cohorts from other populations, which supports the fact that the same approach to interpret/assess disease severity and the same concept of therapeutic window of opportunity can be applicable to the Chinese population.

There are four major reports describing *ABCA4*-associated retinal disease. The four prevalent variants (c.101_106del (p.Ser34-Leu35del); c.2894A>G (p.Asn965Ser); c.6563T>C (p.Phe2188Ser); and c.2424C>G (p.Tyr808Ter)) were different from those of the European population. In addition, the proportions of the types of detected variants were also different; a higher proportion of deleterious variants (43.4%; 92/212) was identified in the Chinese population compared to the ProgStar cohort (29.0%;71/245), although the recruitment criteria can differ. In our study, three null variants: c.1761-2A>G (6/80 alleles, 8%), c.1222C>T (p.Arg408Ter) (4/80 alleles, 5%), and c.2424C>G (p.Tyr808Ter) (3/80 alleles, 4%) account for 16.3% (13/80 alleles) in total, and the association between genotype and phenotype has been revealed. The prevalence of null variants in this cohort is much higher than the European population, which can be considered as founder

alleles; although further genetic analysis utilizing haplotype data is required to conclude this hypothesis. Interestingly, four previous Chinese studies showed some regional differences, although similar features were observed. Three prevalent variants (c.2894A>G (p. Asn965Ser); c.6563T>G (p.Phe2188Ser); and c.101_106del (p. Ser34_Leu35del)) are shared among three out of the four Chinese cohorts, and the first two variants were prevalent in our cohort. On the other hand, the most prevalent variant (c.1761-2A>G) associated with a severe phenotype in our cohort was not listed as a frequently found variant in the other four Chinese cohorts. In most large Chinese cohort studies, patients were recruited without providing any clinical and genetic criteria of STGD1. This recruitment bias should include or exclude severe phenotypes, such as "retinitis pigmentosa."

Three out of the most prevalent six variants in this study were only reported in the Chinese population: c.1761-2A>G; c.2424C>G (p.Tyr808Ter); and c.53G>C (p.Arg18Pro). Founder effects of these three variants can be considered. It is still difficult to conclude the enriched variants in Western China because the allele frequency data of the general population is only available as a cohort of the Western Chinese population.

In the current study, panel-based NGS targeting 36–450 genes have been applied that enables to detect 3–29% in patients with inherited retinal diseases. The advanced screening methods specifically designed for ABCA4 have been developed with a detection rate of 80% or more elsewhere (Cremers, Lee, Collin, & Allikmets, 2020; Jana et al., 2014). However, it is still not perfect for diagnosing patients only by genetic results. The vast phenotypic heterogeneity confounds the phenotypic diagnosis, especially in patients with generalized retinal dysfunction, thus the phenotypic criterion is focusing on the patients with macular atrophy that misses patients with generalized retinal dysfunction. The ProgStar criteria can miss patients with generalized retinal dysfunction with one pathogenic ABCA4 variant; however, we believe the present criteria are most suitable at this moment for a comprehensive diagnosis aiming for treatment.

There are several limitations in this study. First, selection bias at recruitment related to disease severity should be inherent since it is difficult to collect data from genetically affected subjects with good vision who do not visit clinics/hospitals. Second, this cross-sectional retrospective case series study did not include longitudinal data; thus, prospective natural history studies in a larger cohort could provide more accurate information on the disease severity and progression of STGD1. Third, the molecular mechanisms of disease causation for most variants have been unclear, and the clinical effects of variants are not perfectly understood. Further functional analysis is required to conclude the disease causation of each variant. Forth, due to the limited number of subjects, statistical analysis to investigate correlations between the clinical parameters and the particular variants (or genotype groups) were not available in the current study. Fifth, in our cohort, two patients harbor a VUS or likely benign variants for whom genotype grouping was unavailable. The further genetic analysis would help to determine their genotypes with identifying/excluding other candidate variants. Last, the number of our patients was too small to draw conclusions about the genotype–phenotype associations/correlations in such a heterogeneous disease; therefore, larger cohort studies are required for further detailed analyses.

In conclusion, this study, for the first time, illustrated a spectrum of morphological and functional phenotypes and genotypes in a molecularly confirmed large STGD1 cohort in the Chinese population. A different genetic background underlying STGD1 from the Caucasian population was revealed in this study; meanwhile, shared features based on genotype–phenotype associations were determined. These findings delineate the clinical and genetic characteristics of STGD1.

DATA AVAILABILITY STATEMENT

Data available on request from the authors.

ORCID

Kaoru Fujinami https://orcid.org/0000-0003-4248-0033
Shiying Li https://orcid.org/0000-0001-9783-9520

REFERENCES

Allikmets, R., Singh, N., Sun, H., Shroyer, N. F., Hutchinson, A., Chidambaram, A., … Lupski, J. R. (1997). A photoreceptor cell-specific ATP-binding transporter gene (ABCR) is mutated in recessive Stargardt macular dystrophy. *Nature Genetics*, 15(3), 236–246.

Charbel Issa, P., Barnard, A. R., Herrmann, P., Washington, I., & MacLaren, R. E. (2015). Rescue of the Stargardt phenotype in Abca4 knockout mice through inhibition of vitamin A dimerization. *Proceedings of the National Academy of Sciences of the United States of America*, 112(27), 8415–8420.

Chen, Y., Okano, K., Maeda, T., Chauhan, V., Golczak, M., Maeda, A., & Palczewski, K. (2012). Mechanism of all-trans-retinal toxicity with implications for stargardt disease and age-related macular degeneration. *The Journal of Biological Chemistry*, 287(7), 5059–5069.

Cremers, F. P. M., Lee, W., Collin, R. W. J., & Allikmets, R. (2020). Clinical spectrum, genetic complexity and therapeutic approaches for retinal disease caused by ABCA4 mutations. *Progress in Retinal and Eye Research*, 100861. https://doi.org/10.1016/j.preteyeres.2020.100861.

Dan, H., Huang, X., Xing, Y., & Shen, Y. (2019). Application of targeted exome and whole-exome sequencing for Chinese families with Stargardt disease. *Annals of Human Genetics*, 84(2), 177–184.

Fujinami, K., Akahori, M., Fukui, M., Tsunoda, K., Iwata, T., & Miyake, Y. (2011). Stargardt disease with preserved central vision: Identification of a putative novel mutation in ATP-binding cassette transporter gene. *Acta Ophthalmologica*, 89(3), e297–e298.

Fujinami, K., Lois, N., Davidson, A. E., Mackay, D. S., Hogg, C. R., Stone, E. M., … Michaelides, M. (2013). A longitudinal study of stargardt disease: Clinical and electrophysiologic assessment, progression, and genotype correlations. *American Journal of Ophthalmology*, 155(6), 1075–1088 e1013.

Fujinami, K., Lois, N., Mukherjee, R., McBain, V. A., Tsunoda, K., Tsubota, K., … Michaelides, M. (2013). A longitudinal study of Stargardt disease: Quantitative assessment of fundus autofluorescence, progression, and genotype correlations. *Investigative Ophthalmology & Visual Science*, 54(13), 8181–8190.

Fujinami, K., Sergouniotis, P. I., Davidson, A. E., Mackay, D. S., Tsunoda, K., Tsubota, K., … Webster, A. R. (2013). The clinical effect of homozygous ABCA4 alleles in 18 patients. *Ophthalmology*, 120(11), 2324–2331.

Fujinami, K., Sergouniotis, P. I., Davidson, A. E., Wright, G., Chana, R. K., Tsunoda, K., … Webster, A. R. (2013). Clinical and molecular analysis

of Stargardt disease with preserved foveal structure and function. *American Journal of Ophthalmology*, 156(3), 487–501 e481.

Fujinami, K., Singh, R., Carroll, J., Zernant, J., Allikmets, R., Michaelides, M., & Moore, A. T. (2014). Fine central macular dots associated with childhood-onset Stargardt disease. *Acta Ophthalmologica*, 92(2), e157–e159.

Fujinami, K., Strauss, R. W., Chiang, J. P., Audo, I. S., Bernstein, P. S., Birch, D. G., … ProgStar Study, G. (2019). Detailed genetic characteristics of an international large cohort of patients with Stargardt disease: ProgStar study report 8. *The British Journal of Ophthalmology*, 103(3), 390–397.

Fujinami, K., Zernant, J., Chana, R. K., Wright, G. A., Tsunoda, K., Ozawa, Y., … Moore, A. T. (2015). Clinical and molecular characteristics of childhood-onset Stargardt disease. *Ophthalmology*, 122(2), 326–334.

Fujinami, K., Zernant, J., Chana, R. K., Wright, G. A., Tsunoda, K., Ozawa, Y., … Michaelides, M. (2013). ABCA4 gene screening by next-generation sequencing in a British cohort. *Investigative Ophthalmology & Visual Science*, 54(10), 6662–6674.

Fujinami-Yokokawa, Y., Pontikos, N., Yang, L., Tsunoda, K., Yoshitake, K., Iwata, T., … Fujinami, K. (2019). Japan eye genetics consortium OBO. 2019. Prediction of causative genes in inherited retinal disorders from spectral-domain optical coherence tomography utilizing deep learning techniques. *Journal of Ophthalmology*, 2019, 1691064.

Georgiou, M., Kane, T., Tanna, P., Bouzia, Z., Singh, N., Kalitzeos, A., … Michaelides, M. (2020). Prospective cohort Study of childhood-onset Stargardt disease: Fundus autofluorescence imaging, progression, comparison with adult-onset disease, and disease symmetry. *American Journal of Ophthalmology*, 211, 159–175.

Gill, J. S., Georgiou, M., Kalitzeos, A., Moore, A. T., & Michaelides, M. (2019). Progressive cone and cone-rod dystrophies: Clinical features, molecular genetics and prospects for therapy. *The British Journal of Ophthalmology*, 103, 711–720.

Hood, D. C., Bach, M., Brigell, M., Keating, D., Kondo, M., Lyons, J. S., … International Society For Clinical Electrophysiology of V. (2012). ISCEV standard for clinical multifocal electroretinography (mfERG) (2011 edition). *Documenta Ophthalmologica*, 124(1), 1–13.

Hu, F.-Y., J-k, L., Gao, F.-J., Qi, Y.-H., & Wu, J.-H. (2019). ABCA4 gene screening in a Chinese cohort with Stargardt disease: Identification of 37 novel variants. *Frontiers in Genetics*, 10, 773–773.

Hussain, R. M., Ciulla, T. A., Berrocal, A. M., Gregori, N. Z., Flynn, H. W., Jr., & Lam, B. L. (2018). Stargardt macular dystrophy and evolving therapies. *Expert Opinion on Biological Therapy*, 18(10), 1049–1059.

Hussain, R. M., Gregori, N. Z., Ciulla, T. A., & Lam, B. L. (2018). Pharmacotherapy of retinal disease with visual cycle modulators. *Expert Opinion on Pharmacotherapy*, 19(5), 471–481.

Jana, Z., Xie, Y., Carmen, A., Rosa, R. A., Miguel-Angel, L. M., Francesca, S., … Mette, B. (2014). Analysis of the ABCA4 genomic locus in Stargardt disease. *Human Molecular Genetics*, 23(25), 6797.

Jiang, F., Pan, Z., Xu, K., Tian, L., & Li, Y. (2016). Screening of ABCA4 gene in a Chinese cohort with Stargardt disease or cone-rod dystrophy with a report on 85 novel mutations. *Investigative Ophthalmology & Visual Science*, 57(1), 145–152.

K S. (1909). Über familiäre, progressive Degeneration in der Maculagegend des Auges. *Graefe's Archive for Clinical and Experimental Ophthalmology*, 71, 534–550.

Khan, K. N., Kasilian, M., Mahroo, O. A. R., Tanna, P., Kalitzeos, A., Robson, A. G., … Michaelides, M. (2018). Early patterns of macular degeneration in ABCA4-associated retinopathy. *Ophthalmology*, 125(5), 735–746.

Kong, X., Fujinami, K., Strauss, R. W., Munoz, B., West, S. K., Cideciyan, A. V., … ProgStar Study, G. (2018). Visual acuity change over 24 months and its association with foveal phenotype and genotype in individuals with Stargardt disease: ProgStar Study report no. 10. *JAMA Ophthalmology*, 136(8), 920–928.

Kong, X., Strauss, R. W., Michaelides, M., Cideciyan, A. V., Sahel, J. A., Munoz, B., ... ProgStar, S. G. (2016). Visual acuity loss and associated risk factors in the retrospective progression of Stargardt disease Study (ProgStar report no. 2). Ophthalmology, 123(9), 1887–1897.

Kubota, R., Boman, N. L., David, R., Mallikaarjun, S., Patil, S., & Birch, D. (2012). Safety and effect on rod function of ACU-4429, a novel small-molecule visual cycle modulator. Retina, 32(1), 183–188.

Kubota, R., Calkins, D. J., Henry, S. H., & Linsenmeier, R. A. (2019). Emixustat reduces metabolic demand of dark activity in the retina. Investigative Ophthalmology & Visual Science, 60(14), 4924–4930.

Lange, C., Feltgen, N., Junker, B., Schulze-Bonsel, K., & Bach, M. (2009). Resolving the clinical acuity categories "hand motion" and "counting fingers" using the Freiburg visual acuity test (FrACT). Graefe's Archive for Clinical and Experimental Ophthalmology, 247(1), 137–142.

Liu, X., Fujinami, Y. Y., Yang, L., Arno, G., & Fujinami, K. (2019). Stargardt disease in Asian population. In Advances in vision research (Vol. II, pp. 279–295). Singapore: Springer.

Lois, N., Holder, G. E., Bunce, C., Fitzke, F. W., & Bird, A. C. (2001). Phenotypic subtypes of Stargardt macular dystrophy-fundus flavimaculatus. Archives of Ophthalmology, 119(3), 359–369.

Maeda, A., Maeda, T., Golczak, M., & Palczewski, K. (2008). Retinopathy in mice induced by disrupted all-trans-retinal clearance. The Journal of Biological Chemistry, 283(39), 26684–26693.

McBain, V. A., Townend, J., & Lois, N. (2012). Progression of retinal pigment epithelial atrophy in stargardt disease. American Journal of Ophthalmology, 154(1), 146–154.

McCulloch, D. L., Marmor, M. F., Brigell, M. G., Hamilton, R., Holder, G. E., Tzekov, R., & Bach, M. (2015a). Erratum to: ISCEV standard for full-field clinical electroretinography (2015 update). Documenta Ophthalmologica, 131(1), 81–83.

McCulloch, D. L., Marmor, M. F., Brigell, M. G., Hamilton, R., Holder, G. E., Tzekov, R., & Bach, M. (2015b). ISCEV standard for full-field clinical electroretinography (2015 update). Documenta Ophthalmologica, 130(1), 1–12.

Mehat, M. S., Sundaram, V., Ripamonti, C., Robson, A. G., Smith, A. J., Borooah, S., ... Bainbridge, J. W. B. (2018). Transplantation of human embryonic stem cell-derived retinal pigment epithelial cells in macular degeneration. Ophthalmology, 125(11), 1765–1775.

Molday, L. L., Rabin, A. R., & Molday, R. S. (2000). ABCR expression in foveal cone photoreceptors and its role in Stargardt macular dystrophy. Nature Genetics, 25(3), 257–258.

Molday, R. S. (2015). Insights into the molecular properties of ABCA4 and its role in the visual cycle and Stargardt disease. Progress in Molecular Biology and Translational Science, 134, 415–431.

Molday, R. S., Zhong, M., & Quazi, F. (2009). The role of the photoreceptor ABC transporter ABCA4 in lipid transport and Stargardt macular degeneration. Biochimica et Biophysica Acta, 1791(7), 573–583.

Quazi, F., Lenevich, S., & Molday, R. S. (2012). ABCA4 is an N-retinylidene-phosphatidylethanolamine and phosphatidylethanolamine importer. Nature Communications, 3, 925.

Rahman, N., Georgiou, M., Khan, K. N., & Michaelides, M. (2020). Macular dystrophies: Clinical and imaging features, molecular genetics and therapeutic options. The British Journal of Ophthalmology, 104(4), 451–460.

Richards, S., Aziz, N., Bale, S., Bick, D., Das, S., Gastier-Foster, J., ... Committee, A. L. Q. A. (2015). Standards and guidelines for the interpretation of sequence variants: A joint consensus recommendation of the American College of Medical Genetics and Genomics and the Association for Molecular Pathology. Genetics in Medicine, 17(5), 405–424.

Rosenfeld, P. J., Dugel, P. U., Holz, F. G., Heier, J. S., Pearlman, J. A., Novack, R. L., ... Kubota, R. (2018). Emixustat hydrochloride for geographic atrophy secondary to age-related macular degeneration: A randomized clinical trial. Ophthalmology, 125(10), 1556–1567.

Sasso, P., Scupola, A., Silvestri, V., Amore, F. M., Abed, E., Calandriello, L., ... Caporossi, A. (2017). Morpho-functional analysis of Stargardt disease for reading. Canadian Journal of Ophthalmology, 52(3), 287–294.

Schonbach, E. M., Strauss, R. W., Ibrahim, M. A., Janes, J. L., Birch, D. G., Cideciyan, A. V., ... ProgStar study g. (2020). Faster sensitivity loss around dense scotomas than for overall macular sensitivity in Stargardt disease: ProgStar report no. 14. American Journal of Ophthalmology, 216, 219–225.

Schonbach, E. M., Wolfson, Y., Strauss, R. W., Ibrahim, M. A., Kong, X., Munoz, B., ... ProgStar Study, G. (2017). Macular sensitivity measured with microperimetry in Stargardt disease in the progression of atrophy secondary to Stargardt disease (ProgStar) study: Report no. 7. JAMA Ophthalmology, 135(7), 696–703.

Schulz, H. L., Grassmann, F., Kellner, U., Spital, G., Ruther, K., Jagle, H., ... Stohr, H. (2017). Mutation spectrum of the ABCA4 gene in 335 Stargardt disease patients from a multicenter German cohort-impact of selected deep Intronic variants and common SNPs. Investigative Ophthalmology & Visual Science, 58(1), 394–403.

Schwartz, S. D., Hubschman, J. P., Heilwell, G., Franco-Cardenas, V., Pan, C. K., Ostrick, R. M., ... Lanza, R. (2012). Embryonic stem cell trials for macular degeneration: A preliminary report. Lancet, 379(9817), 713–720.

Schwartz, S. D., Regillo, C. D., Lam, B. L., Eliott, D., Rosenfeld, P. J., Gregori, N. Z., ... Lanza, R. (2015). Human embryonic stem cell-derived retinal pigment epithelium in patients with age-related macular degeneration and Stargardt's macular dystrophy: Follow-up of two open-label phase 1/2 studies. Lancet, 385(9967), 509–516.

Singh, R., Fujinami, K., Chen, L. L., Michaelides, M., & Moore, A. T. (2014). Longitudinal follow-up of siblings with a discordant Stargardt disease phenotype. Acta Ophthalmologica, 92(4), e331–e332.

Strauss, R. W., Ho, A., Munoz, B., Cideciyan, A. V., Sahel, J. A., Sunness, J. S., ... Progression of Stargardt Disease Study G. (2016). The natural history of the progression of atrophy secondary to Stargardt disease (ProgStar) studies: Design and baseline characteristics: ProgStar report no. 1. Ophthalmology, 123(4), 817–828.

Strauss, R. W., Kong, X., Ho, A., Jha, A., West, S., Ip, M., ... ProgStar Study, G. (2019). Progression of Stargardt disease as determined by fundus autofluorescence over a 12-month period: ProgStar report no. 11. JAMA Ophthalmology, 137, 1134.

Strauss, R. W., Munoz, B., Ho, A., Jha, A., Michaelides, M., Cideciyan, A. V., ... ProgStar Study, G. (2017a). Progression of Stargardt disease as determined by fundus autofluorescence in the retrospective progression of Stargardt disease Study (ProgStar report no. 9). JAMA Ophthalmology, 135(11), 1232–1241.

Strauss, R. W., Munoz, B., Ho, A., Jha, A., Michaelides, M., Mohand-Said, S., ... ProgStar Study, G. (2017b). Incidence of atrophic lesions in Stargardt disease in the progression of atrophy secondary to Stargardt disease (ProgStar) study: Report no. 5. JAMA Ophthalmology, 135(7), 687–695.

Tanna, P., Georgiou, M., Aboshiha, J., Strauss, R. W., Kumaran, N., Kalitzeos, A., ... Michaelides, M. (2018). Cross-sectional and longitudinal assessment of retinal sensitivity in patients with childhood-onset Stargardt disease. Translational Vision Science & Technology, 7(6), 10.

Tanna, P., Georgiou, M., Strauss, R. W., Ali, N., Kumaran, N., Kalitzeos, A., ... Michaelides, M. (2019). Cross-sectional and longitudinal assessment of the ellipsoid zone in childhood-onset Stargardt disease. Translational Vision Science & Technology, 8(2), 1.

Tanna, P., Strauss, R. W., Fujinami, K., & Michaelides, M. (2017). Stargardt disease: Clinical features, molecular genetics, animal models and therapeutic options. The British Journal of Ophthalmology, 101(1), 25–30.

Testa, F., Melillo, P., Di Iorio, V., Orrico, A., Attanasio, M., Rossi, S., & Simonelli, F. (2014). Macular function and morphologic features in juvenile stargardt disease: Longitudinal study. *Ophthalmology*, *121*(12), 2399–2405.

Tsybovsky, Y., Molday, R. S., & Palczewski, K. (2010). The ATP-binding cassette transporter ABCA4: Structural and functional properties and role in retinal disease. *Advances in Experimental Medicine and Biology*, *703*, 105–125.

Xin, W., Xiao, X., Li, S., Jia, X., Guo, X., & Zhang, Q. (2015). Identification of genetic defects in 33 Probands with Stargardt disease by WES-based bioinformatics gene panel analysis. *PLoS One*, *10*, e0132635.

SUPPORTING INFORMATION

Additional supporting information may be found online in the Supporting Information section at the end of this article.